Proceedings of the ASME 2021 16th International Manufacturing Science and Engineering Conference
MSEC2021
June 21-25, 2021, Cincinnati, OH, USA

MSEC2021-60409

THE FDTD ANALYSIS OF NEAR-FIELD RESPONSE FOR MICROGROOVE STRUCTURE WITH STANDING WAVE ILLUMINATION FOR THE REALIZATION OF COHERENT STRUCTURED ILLUMINATION MICROSCOPY

Yizhao Guan[1], Hiromasa Kume[1], Shotaro Kadoya[1], Masaki Michihata[1], Satoru Takahashi[1]

[1]The University of Tokyo, Tokyo, Japan

ABSTRACT

Microstructures are widely used in the manufacture of functional surfaces. An optical-based super-resolution, non-invasive method is preferred for the inspection of surfaces with massive microstructures. The Structured Illumination Microscopy (SIM) uses standing-wave illumination to reach optical super-resolution. Recently, coherent SIM is being studied. It can obtain not only the super-resolved intensity distribution but also the phase and amplitude distribution of the sample surface beyond the diffraction limit. By analysis of the phase-depth dependency, the depth measurement for microgroove structures with coherent SIM is expected. FDTD analysis is applied for observing the near-field response of microgroove under the standing-wave illumination. The near-field phase shows depth dependency in this analysis. Moreover, the effects from microgroove width, the incident angle, and the relative position between the standing-wave peak and center of the microgroove are investigated. It is found the near-field phase change can measure depth until 200 nm (aspect ratio 1) with an error of up to 20.4 nm in the case that the microgroove width is smaller than half of the wavelength.

Keywords: Structured Illumination microscopy, FDTD, depth measurement

1. INTRODUCTION

Nowadays, fabricating microstructures among the material surface provides specific functions. For example, the antireflection coating can be fabricated by modifying the surface. Subwavelength textured structures provide the equivalent effect of infinite layers of antireflective thin films to further reduce the reflectance.[1] Another example is the microfluidic systems. Microfluidic systems have applications ranging from biology to energy and can integrate assay operations such as detection and sample pre-preparation on one chip.[2] Functional surfaces are manufactured based on arrangements of nanochannels, as shown in Figure 1. A typical fundamental element is a microgroove. With the miniaturization, the width and depth are on the scale of the nanometer. The inspection of manufactured microstructures is necessary for the correct functioning of the functional surfaces. In the inspection process, depth measurement is as crucial as width measurement. In optical super-resolution researches,

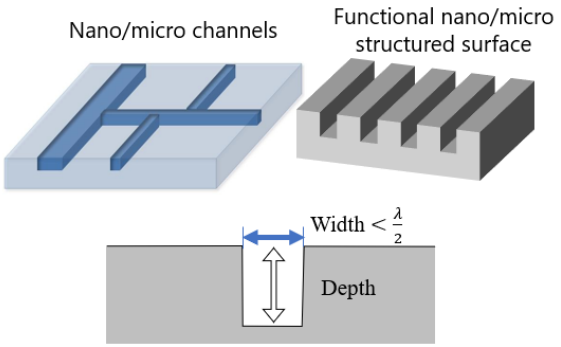

FIGURE 1: Functional surface with microgroove structure such as nanochannels, periodic structures, optical devices and so on.

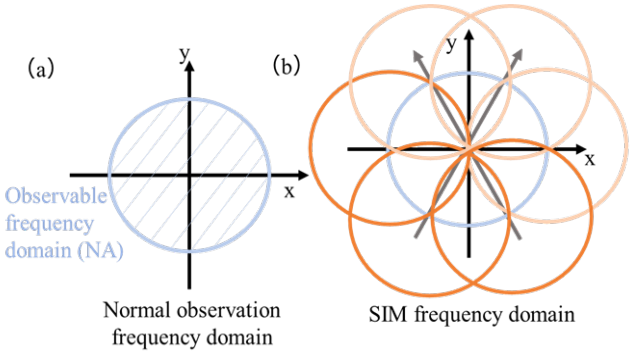

FIGURE 2: SIM enlarges the observable region (from (a) to (b)) in frequency domain to reach super-resolution by phase shift three times along one axis. For a two-dimensional super-resolution, shifts are done in three axes rotated $\frac{\pi}{3}\ rad$ in this case

multiple methods breaking the Rayleigh limit to conduct measurement on the level of ~ 100 nm have been proposed for width measurement, while the super-resolution for depth measurement is desirable as well. This study focuses on depth measurement with optical super-resolution methods.

The optical methods have the advantage of high throughput and non-invasiveness comparing to others. For example, Atomic Force Microscopy (AFM) and cross-section Scanning Electron Microscopy (SEM) can be used to profile microgrooves in three dimensional. However, AFM requires a scanning process while cross-section SEM has to dismantle the sample. Therefore, a three-dimensional super-resolution optical method is desirable for the inspection of microgrooves' quality.

The structured illumination microscopy (SIM) is one of the developed optical super-resolution methods. SIM utilize structured light pattern. Typical illumination is the standing-wave illumination formed by two oblique monochrome incidences in opposite directions to form a Moiré pattern. The optical resolution is limited by the Numerical Aperture (NA). In the frequency domain that NA creates a cutoff area in the observable frequency region. It is mathematically possible to compute the unknown frequency content around the cutoff area through the SIM reconstruction algorithm.[3] Three times phase shifts (two more figures beside the original one) are necessary. The phase shift of incident light leads to the peak shift of the standing-wave in real space, and it provides more information near the initial cutoff area in the frequency domain. The illustration is in Figure 2. As a result, the SIM can obtain a two-dimensional optical super-resolution. However, for super-resolution of both width and depth, an improvement should be developed for the SIM reconstruction algorithm to achieve three-dimensional super-resolution.

Moreover, the coherent SIM algorithm is under development recently, as shown in Figure 3. Not only the intensity of response but also the phase and amplitude will be obtained with this new algorithm, compared to the previous incoherent SIM algorithm.[4] The principle of coherent SIM is explained. Since the coherent information can not be obtained directly from the Charge-Coupled Device (CCD), a reference light is introduced into SIM's illumination system to interfere with the scattering light from the sample. The images obtained with interference can calculate the phase of scattering light.

On the other hand, the interferometer utilizes the phase change of the reflected light from the sample surface to measure its depth. A similar principle may also be available in the case of standing-wave illumination based on coherent SIM. Therefore, it becomes indispensable to study the phase and microgroove depth relationship under standing-wave illumination. Finite-Difference Time-Domain method (FDTD) is applied.

2. MODEL AND METHODOLOGY

The model is built with a microgroove set at the center with depth variance in Figure 4. The software used is Poynting developed by Fujitsu. The parameters and boundary conditions are shown in table 1. Periodic Boundary Condition (PBC) is set in x-direction and z-direction, and Perfect Matched Layer (PML) absorption boundary condition is set in the y-direction. The light source is set beyond the microgroove while keeping enough spacing, and two oblique incident light form the standing-wave illumination. The microgroove is set in the middle of the model. It is found that when the microgroove width is smaller than the wavelength, the TE wave can not reach the bottom of the microgroove while TM wave can. Therefore, the polarization is set in the x-direction. The material of the microgroove is silicon.

In Figure 5, The time average of the electric field shows that the standing-wave exists in both x and y-direction. It is the x-components of two oblique incidences form the standing-wave in the x-direction. The incidence and reflection propagate in opposite directions forming the standing-wave in the y-direction. The constructive interference forms peaks while the destructive interference forms nodes. By manipulating one of the oblique incident light initial phase, the standing-wave and microgroove shift their relative position. The light reached the bottom of the microgroove in Figure 5(a) when the standing-wave peak is above the microgroove. On the other hand, the shift of standing-wave peak by $\frac{1}{4}\lambda$ is shown in Figure 5(b).

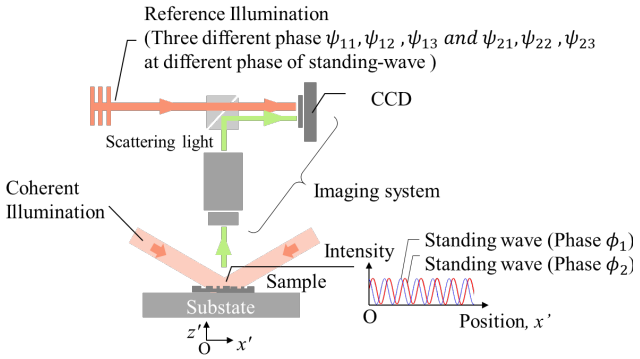

FIGURE 3: Coherent SIM with its illumination process [4]

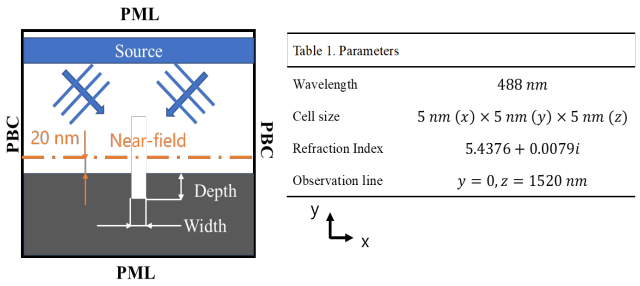

Table 1. Parameters

Wavelength	488 nm
Cell size	5 nm (x) × 5 nm (y) × 5 nm (z)
Refraction Index	$5.4376 + 0.0079i$
Observation line	$y = 0, z = 1520\ nm$

y
x

FIGURE 4: Set up and parameters for FDTD analysis

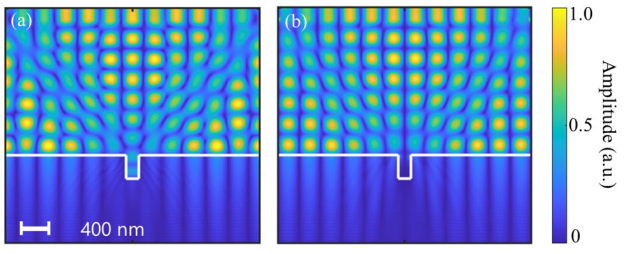

FIGURE 5: Time average of electric field when standing-wave peak is above the microgroove (a), and when standing-wave is shifted by $\frac{1}{4}\lambda$ and its node is above the microgroove (b)

Subtraction between the model with an air model is conducted to extract the near-field optical response from the microgroove surface. This process removes the effect of the light source.

The phase is obtained at near-field by setting an observer line $20\,nm$ above the surface so that the disturbance from adjacent microgrooves can be suppressed. The endeavor should be made in further research to reconstruct near-field phase information from far-field phase and amplitude in practical application. According to the perpendicular illumination interferometer, in previous research, Ye. etc., has established far-field based near-field reconstruction depth measurement (FNRDM). [5]

A typical phase and intensity for standing-wave obtained from the observer in the x-direction are shown in Figure 6. The microgroove is illuminated by light with this unique characteristic, and its phase change introduced by depth change is the key to the development of optical nanoscale depth measurement. The phase-depth dependency and relative position of phase and microgroove has been investigated.

3. RESULTS AND DISCUSSION

Firstly, the phase of optical response from flat silicon is plotted in Figure 7(a), where the standing-wave like behaviors of phase is confirmed. Though the phase distribution near boundary is disturbed by calculation errors, the phase area of interest between $-1300\,nm$ and $1300\,nm$ is close to the illustration of the standing-wave. A microgroove depth dependency is observed in Figure 7(b) when the width of the microgroove is $3000\,nm$, which is considered to be much larger than the wavelength of $488\,nm$. The phase at the center above the microgroove changes monotonically with depth.

Moreover, the simulation region in the width direction is large enough to ensure no apparent interaction between two adjacent microgrooves in the periodic boundary condition so that the phase change is only depth-dependent. Phase variances can be observed at the edge of the microgroove at $\pm 1500\,nm$. By setting the standard phase at zero depth as in Figure 7(a), we can obtain the phase change with depth. The sampling point of the near-field phase is the same as in Figure 7(b). The phase change is unwrapped manually by adding 2π for data from depths deeper than $210\,nm$ when a sudden jump occurs, as shown in Figure 8.

Secondly, the incident angle has been swept for standing-wave. The different slope has been observed with incident angle variance. It can be explained by the equation (1) for the oblique interferometer

$$Depth = \frac{\lambda}{2} \times (\theta_n / 2\pi + k) \times cos\,(\phi) \qquad (1)$$

Where θ_n is the phase difference, ϕ is the incident angle, and k is an integer.

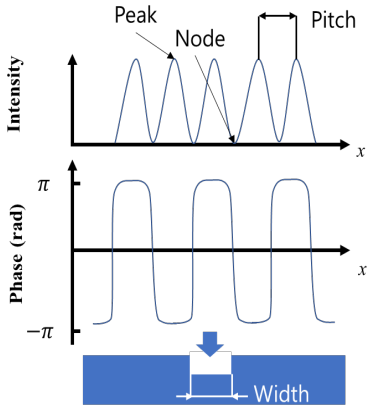

FIGURE 6: An illustration for the near-field intensity and phase of the standing-wave illumination. This light interact with the microgroove structure and its response with width variance is the key of depth measurement

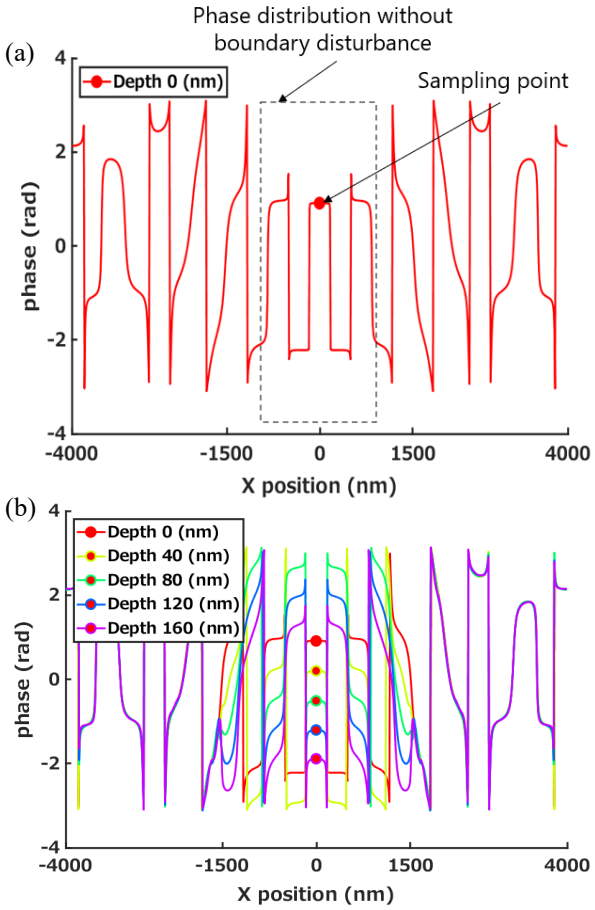

FIGURE 7: Near-field phase response obtained from FDTD when the incident angle is $45\,degree$, microgroove width is $3000\,nm$, and the standing-wave peak is at the center above microgroove. (a) Response from a flat silicon surface, and the phase at 0 in x position is taken as standard phase to calculate the phase difference. The rectangular area of interest shows a typical standing-wave phase (b) Phase varies with depth

It is found that the oblique interference theory matches numerical results in the standing-wave illumination case when the microgroove is much larger than the illumination wavelength. The results are shown in Figure 9, where dots present the FDTD results, and solid lines are theoretical values from equation (1).

Then, the width has been reduced in Figure 9 because the microstructure of width smaller than the Rayleigh limit is the primary concern of this research. Results show that the microgroove width affects phase-depth dependency. It appears that when the width approaches the wavelength, a disturbance is introduced to deviate the FDTD data from oblique interferometer theory. The deviation is more significant at a larger incident angle. It indicates that a separate mechanism dominates when the incident angle is large since less light can achieve the bottom of the microgroove at a larger incident angle.

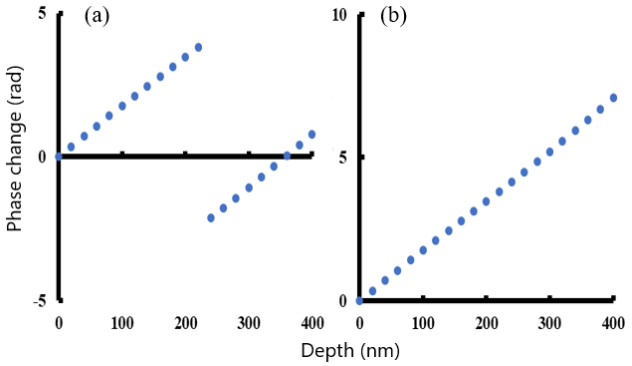

FIGURE 8: Before (a) and after (b) the phase unwrapping for near-field phase difference and depth relationship obtained from FDTD when the incident angle is $45\ degree$, microgroove width is $3000\ nm$, and the standing-wave peak is at the center above microgroove

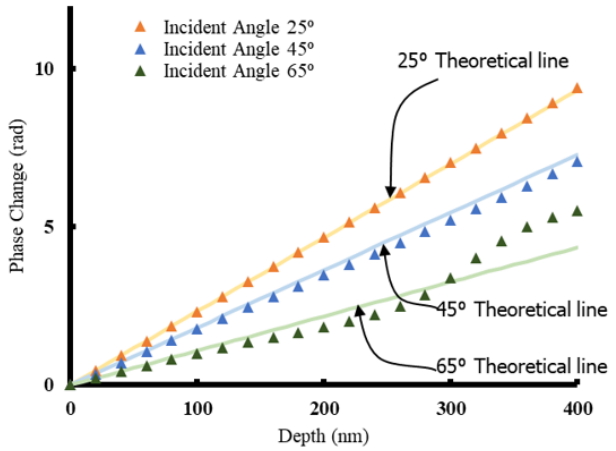

FIGURE 9: Near-field phase response obtained from FDTD when microgroove width is $3000\ nm$, and the standing-wave peak is at the center above microgroove. The solid line is the phase-depth relation calculated from equation (1).

Next, Figure 10 shows the relationship between phase and depth when the width of the microgroove is $200\ nm$. Analysis indicates that the depth and relative phase change relationship becomes independent with the incident angle. This new linear relationship is similar to the case with the perpendicular illumination interferometer of 0 incident angle.

Finally, the standing-wave peak position is studied in Figure 10. Since SIM needs three images (with two shifts from the original position) to achieve two-dimensional super-resolution, the relative position of standing-wave peak and microgroove becomes essential. The peak shift has been swept for $0, \frac{1}{8}\lambda, \frac{1}{4}\lambda, \frac{1}{2}\lambda$. The phase does not change with the depth when the node of standing-wave intensity overlaps the microgroove center, which is the sampling point.

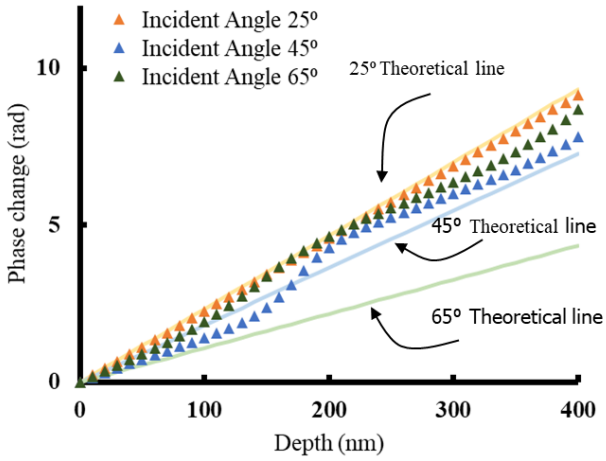

FIGURE 10: Near-field phase response obtained from FDTD when microgroove width is $1000\ nm$, and the standing-wave peak is at the center above microgroove. The solid line is the phase-depth relation calculated from equation (1).

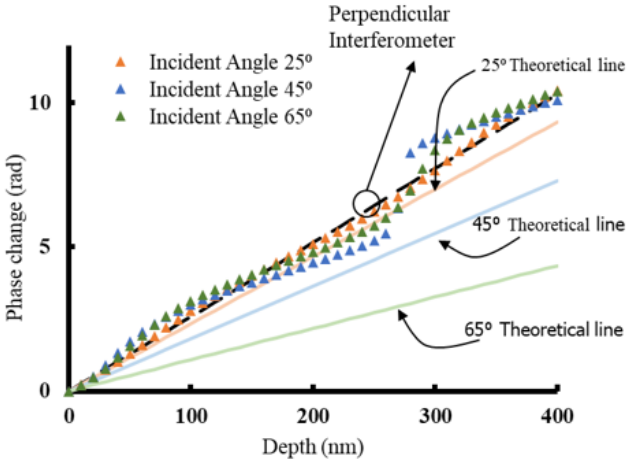

FIGURE 11: Near-field phase difference and depth relationship obtained from FDTD when the microgroove width is $200\ nm$, and the standing-wave peak is at the center above microgroove. The solid line is theoretical value when incident angle is 0.

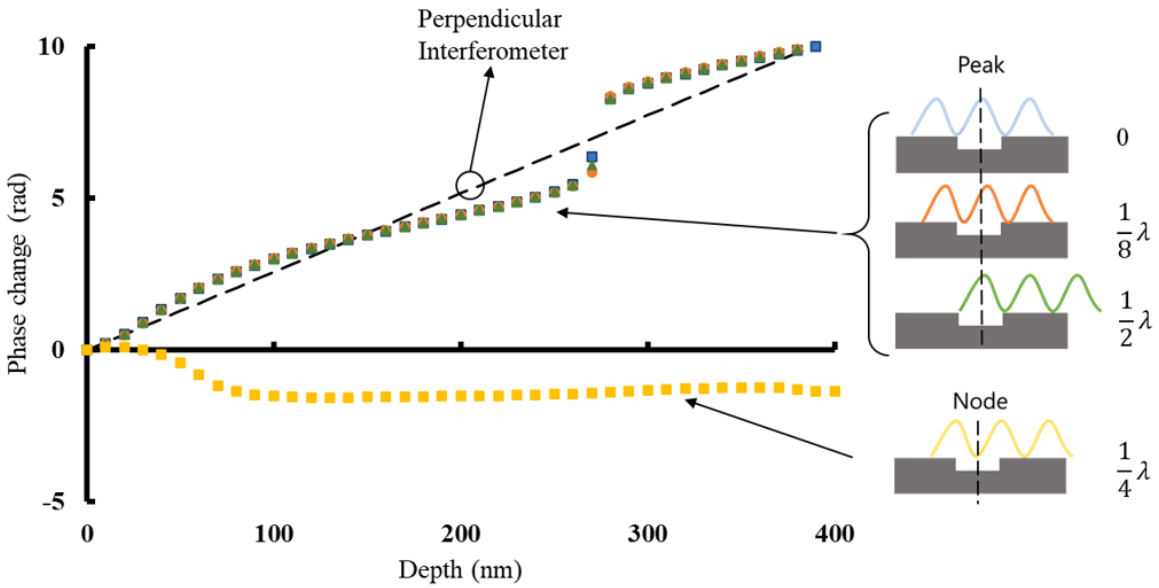

FIGURE 12: The relative position of standing-wave and microgroove does not affect the near-field phase difference and depth relationship obtained from FDTD except the case that the node region is above the microgroove. The microgroove width is $200\ nm$, and the incident angle is 45 degrees.

4. Discussion

Firstly, the oblique incidence interferometer theory can explain the phase-depth relationship obtained from FDTD analysis for the model with standing-wave illumination when the width of the microgroove can be considered to be wide enough comparing to the wavelength. The reason is that the interaction of microgroove edges and incident light does not affect the oblique interferometer theory, which assumes the light behaves in a beam way.

Furthermore, it is revealed that a new mechanism dominates when the microgroove's width is smaller than half of the wavelength. The perpendicular illuminating interferometer theory may explain this phase-depth relationship. The reason behind this can be considered as the waveguide-like behavior dominates. A particular phase pattern propagates perpendicular inside the microgroove as it follows a certain propagation mode, which is affected by polarization, wavelength, incident angle, and microgroove width. The phase pattern keeps almost the same during its propagation. This phase pattern response can bring back the depth information so that the phase difference detected is related to perpendicular interferometer theory.

Finally, the phase-depth dependency invalidates when the phase sampling point overlaps the standing-wave intensity node because the noise effect can not be ignored when the light intensity is too weak. The region that is not suitable for phase measurement is $\pm 0.0038\lambda$.

5. CONCLUSION

The results obtained by FDTD analysis in this paper are summarized as follows.

Firstly, the near-field phase varies with the depth of microgroove under standing-wave illumination. This correlation can be obtained even that the microgroove width is smaller than the wavelength. It is revealed that the microgroove's width compared to the wavelength leads to a different mechanism of this variation. The variation follows the perpendicular incident interferometer theory in a narrow width case even under the oblique incidence, while it follows the oblique incident interferometer theory at a wide width. For microgroove with $200\ nm$ width, the near-field phase change can measure depth until $200\ nm$ (aspect ratio 1) with an error of up to $20.4\ nm$.

Secondly, analysis of changing standing-wave illumination peak shift reveals that the phase-depth relationship valid except when the standing-wave node region ($\pm 0.0038\lambda$) overlaps the sampling point.

These results suggest that adding one more peak shift of standing-wave illumination to avoid the problem allows the realization of the coherent SIM, and that the phase measurement obtained by the coherent SIM can calculate the depth of microgroove with aspect ratio 1, which has width smaller than half wavelength, up to about 10% error.

For future work, the precision and applicable width and depth of this proposed method will be discussed further with analysis based on waveguide theory.

ACKNOWLEDGEMENTS

This work was supported by JSPS KAKENHI Grant Numbers JP19H02036.

REFERENCES

[1] Kim, Kyunghwan, Yunwon Song, and Jungwoo Oh. "Nano/micro dual-textured antireflective subwavelength structures in anisotropically etched GaAs." Optics letters 42.16 (2017): 3105-3108.

[2] Matschuk, Maria, Henrik Bruus, and Niels B. Larsen. "Nanostructures for all-polymer microfluidic systems." *Microelectronic Engineering* 87.5-8 (2010): 1379-1382.

[3] Lal, Amit, Chunyan Shan, and Peng Xi. "Structured illumination microscopy image reconstruction algorithm." *IEEE Journal of Selected Topics in Quantum Electronics* 22.4 (2016): 50-63.

[4] H. Kume, M. Michihata, K. Takamasu, S. Takahashi. Numerical analysis on high resolution optical measurement method with long working distance objective for in-line inspection of micro-structured surface, *Precision Engineering*. (2020)

[5] Ye, Shiwei, et al. "Modified Linnik microscopic interferometry for quantitative depth evaluation of diffraction-limited microgroove." *Measurement Science and Technology* 29.5 (2018): 054011.